Cancer Cell
Article

CH5424802, a Selective ALK Inhibitor Capable of Blocking the Resistant Gatekeeper Mutant

Hiroshi Sakamoto,[1,*] Toshiyuki Tsukaguchi,[1] Sayuri Hiroshima,[2] Tatsushi Kodama,[1] Takamitsu Kobayashi,[1] Takaaki A. Fukami,[1] Nobuhiro Oikawa,[1] Takuo Tsukuda,[1] Nobuya Ishii,[1] and Yuko Aoki[1]
[1]Kamakura Research Laboratories, Chugai Pharmaceutical Co., Ltd.
[2]Chugai Research Institute for Medical Science, Inc.
200 Kajiwara, Kamakura, Kanagawa 247-8530, Japan
*Correspondence: sakamotohrs@chugai-pharm.co.jp
DOI 10.1016/j.ccr.2011.04.004

SUMMARY

Anaplastic lymphoma kinase (ALK) is a tyrosine kinase that is constitutively activated in certain cancers, following gene alterations such as chromosomal translocation, amplification, or point mutation. Here, we identified CH5424802, a potent, selective, and orally available ALK inhibitor with a unique chemical scaffold, showing preferential antitumor activity against cancers with gene alterations of ALK, such as nonsmall cell lung cancer (NSCLC) cells expressing EML4-ALK fusion and anaplastic large-cell lymphoma (ALCL) cells expressing NPM-ALK fusion in vitro and in vivo. CH5424802 inhibited ALK L1196M, which corresponds to the gatekeeper mutation conferring common resistance to kinase inhibitors, and blocked EML4-ALK L1196M-driven cell growth. Our results support the potential for clinical evaluation of CH5424802 for the treatment of patients with ALK-driven tumors.

INTRODUCTION

Genetic alterations, such as point mutation, chromosomal translocation, and gene amplification, have been identified in various cancers by molecular profiling studies. In clinical studies the remarkable success of targeted protein kinase inhibitors has highlighted the importance of identifying genotype-specific subsets of patients to guide the appropriate selection of targeted therapies. On the other hand, certain factors limit the efficacy of cancer therapies owing to a narrow therapeutic index caused by blocking of multiple kinases related to the regulation of normal cell growth. A second-generation BCR-ABL inhibitor, nilotinib, is a more potent and selective inhibitor of BCR-ABL than imatinib (Weisberg et al., 2005). A recent clinical trial revealed that nilotinib was superior to imatinib against newly diagnosed BCR-ABL-positive chronic myelogenous leukemia (CML) (Saglio et al., 2010), suggesting that more potent and selective kinase inhibitors needed to be developed in order to achieve higher efficacy and safety.

Acquired resistance to kinase inhibitors is one of the most serious problems in long-term cancer treatment; this is caused by various mechanisms, such as gene alterations of the target molecules or other gene alterations. In the majority of cases, it results from the selection of cancer cells with point mutations in the kinase catalytic domain of target genes such as *ABL* or *EGFR* (Branford et al., 2002; Pao et al., 2005). Among the point mutations in the kinase domain, the gatekeeper-residue mutation is known to be commonly involved in resistance to kinase inhibitors. Based on a recent structural analysis of the kinase domain, AP24534 was shown to inhibit the BCR-ABL T315I gatekeeper mutant (O'Hare et al., 2009). Furthermore, irreversible EGFR inhibitors have been shown to overcome the acquired resistance by the T790M-resistant mutation of EGFR (Zhou et al., 2009; Sos et al., 2010). Thus, kinase inhibitors retaining the inhibitory potency against the gatekeeper mutants would confer various advantages in longer-term cancer treatment.

EML4-ALK has been identified as a fusion oncogene in nonsmall cell lung cancer (NSCLC) (Soda et al., 2007). The

Significance

The recent development of targeted protein kinase inhibitors has provided opportunities in cancer treatment. However, certain factors limit the efficacy of cancer therapies, such as a narrow therapeutic index caused by inhibition of multiple kinases, and the emergence of resistant mutants. CH5424802 has been demonstrated to be an ALK inhibitor with high selective properties, and potential antitumor activity against the gatekeeper mutant L1196M in EML4-ALK, which was clinically confirmed in tumor cells isolated from a patient with NSCLC who was refractory to the c-MET/ALK inhibitor, PF-02341066 (crizotinib). Potent ALK inhibitors effective against the gatekeeper mutants may offer clinical advantages in cancer treatment for patients with ALK-driven tumors.

tumorigenic potential of EML4-ALK was subsequently confirmed using a transformation assay via the subcutaneous (s.c.) injection of transfected 3T3 fibroblasts into mice (Soda et al., 2007) and the transgenic mice (Soda et al., 2008). *EML4-ALK* positivity was shown to be associated with resistance to EGFR tyrosine kinase inhibitors among patients with metastatic NSCLC (Rodig et al., 2009). Moreover, multiple variants of EML4-ALK (Choi et al., 2008; Takeuchi et al., 2008) and other oncokinase fusions such as KIF5B-ALK (Takeuchi et al., 2009) have also been identified in NSCLC. In addition to NSCLC, anaplastic lymphoma kinase (ALK) fusion proteins have been identified in anaplastic large-cell lymphoma (ALCL) (Morris et al., 1994) and inflammatory myofibroblastic tumors (IMTs) (Griffin et al., 1999). Gene amplification or point mutation of *ALK* was demonstrated to be in the oncogenesis of neuroblastoma (Chen et al., 2008; George et al., 2008; Janoueix-Lerosey et al., 2008; Mossé et al., 2008). Because the growth of these tumors is strongly addicted to ALK activity, suppression of ALK could be a potent therapeutic strategy for patients with gene alterations of *ALK*. Small-molecule ALK inhibitors have not yet been approved as anticancer agents. PF-02341066 (Christensen et al., 2007), an inhibitor of c-MET and ALK, showed a high response rate in patients with NSCLC with *ALK* rearrangement in clinical trial (Kwak et al., 2010), and it is currently under phase III clinical development. Meanwhile, a recent report described the identification of *EML4-ALK* C1156Y and L1196M mutations by genetic analysis using a pleural-effusion specimen from a patient with NSCLC who relapsed after a partial response to PF-02341066 in clinical trial, suggesting that L1196M and C1156Y mutation confer clinical resistance to ALK inhibitors (Choi et al., 2010). Additionally, F1174L mutation was identified as one of the causes of PF-02341066 resistance in a patient with an IMT harboring an *RANBP2-ALK* translocation who progressed while on PF-02341066 (Sasaki et al., 2010). Thus, the development of ALK inhibitors with effectiveness to resistant mutants would be needed.

RESULTS

Potent and Selective Inhibition of ALK Activity of CH5424802

In order to differentiate from other described ALK inhibitors, we focused on identifying a more selective ALK inhibitor. We have performed high-throughput inhibitor screening against multiple cancer-related tyrosine kinase targets and obtained several hits with previously unreported chemical scaffolds. Among the derivatives we found a lead compound that strongly inhibits ALK; subsequently, we intensively modified and improved its kinase selectivity and pharmacokinetics profile. Finally, we identified a benzo[*b*]carbazole derivative, CH5424802, as a potent, selective, and orally available ALK inhibitor (Figure 1A). In cell-free assays the IC_{50} of CH5424802 for enzyme activity of ALK was 1.9 nM (Table 1; see Table S1 available online); the dissociation constant (K_D) value for ALK in an ATP-competitive manner was 2.4 nM using a competition-binding assay (Ambit). The inhibitory activity for two hot spot-activating mutations in neuroblastoma, F1174L and R1275Q, was comparable to that for wild-type ALK (Table 1). To explore the kinase selectivity of CH5424802, its inhibitory activity on various kinases was measured, revealing weak or no inhibition against 24 protein kinases other than ALK (Table 1). Furthermore, using Ambit's kinase screening platform, CH5424802 was profiled against 402 kinases including the mutated kinases. Only three kinases, ALK, GAK, and LTK, showed more than 50% inhibition at 10 nM, which corresponds to approximately 5-fold higher concentration of IC_{50} values for ALK (Table S2). LTK is known to show greatest sequence similarity to ALK (Iwahara et al., 1997). In cellular phosphorylation assays, CH5424802 could prevent autophosphorylation of ALK in NCI-H2228 NSCLC cells expressing EML4-ALK (Figure 1B), and it also resulted in substantial suppression of phosphorylation of STAT3 and AKT, but not of ERK1/2. However, inhibition of these phosphorylations was not observed in ALK fusion-negative A549 cell line (Figure S1A).

Selective Antitumor Activity in ALK-Positive Cancers

In NSCLC, EML4-ALK fusion has been shown to be mutually exclusive with EGFR or KRAS mutations (Inamura et al., 2008). It has also been reported that EGFR tyrosine kinase inhibitors have high clinical efficacy as therapeutic agents for NSCLCs with EGFR mutations (Pao et al., 2004). Using NSCLC cell lines with distinct genotypes, we tested the antiproliferative effects of CH5424802. CH5424802 was preferentially efficacious against NCI-H2228 cells expressing EML4-ALK, but not ALK fusion-negative NSCLC cell lines, including HCC827 cells (*EGFR* exon 19 deletion), A549 cells (*KRAS* mutant), or NCI-H522 cells (*EGFR* wild-type, *KRAS* wild-type, and *ALK* wild-type) in monolayer culture (Figure 1C; Table S3). Similar results were obtained under three-dimensional (3D) spheroid culture conditions (NCI-H2228, IC_{50} = 33 nM) (Figure 1D). CH5424802 could induce an apoptotic marker—caspase-3/7-like activation—in NCI-H2228 spheroid cells (Figure 1E), indicating the involvement of apoptosis induction in the antitumor activity of CH5424802. The caspase-3/7-like activation was also observed in a treatment of other ALK inhibitors, PF-02341066 and NVP-TAE684, under spheroid culture conditions (Figure S1B). Additionally, we confirmed that EGFR mutant HCC827 cells showed higher sensitivity to the EGFR kinase inhibitor gefitinib, but not to CH5424802 (Figure 1D, middle panel). To evaluate the sensitivity of cell lines with gene alterations of *ALK* other than NSCLC, we performed in vitro cell growth inhibition assays using human lymphoma and neuroblastoma cell lines. CH5424802 inhibited the growth of two lymphoma lines, KARPAS-299 and SR, with NPM-ALK fusion protein but did not affect the growth of an HDLM-2 lymphoma line without ALK fusion (Table S3). Among neuroblastoma lines, NB-1 cells contain amplified *ALK* (Chen et al., 2008), whereas KELLY cells harbor the ALK-activating F1174L point mutation (George et al., 2008). These two neuroblastoma lines with genetic alterations of *ALK* were sensitive to CH5424802, but the wild-type line SK-N-FI was not (Table S3). To further confirm the kinase selectivity in cells, we examined the sensitivity of cell lines with alterations in kinase genes, which are susceptible to the corresponding kinase inhibitors (e.g., c-MET inhibitors for *c-MET* gene amplification). CH5424802 was not efficacious against *c-MET*-, *FGFR2*-, or *ERBB2*-amplified cancer cell lines (Table S3). On the other hand, *c-MET*-amplified cancer cell lines were reported to show high sensitivity to a c-MET inhibitor (Smolen et al., 2006). These results indicated

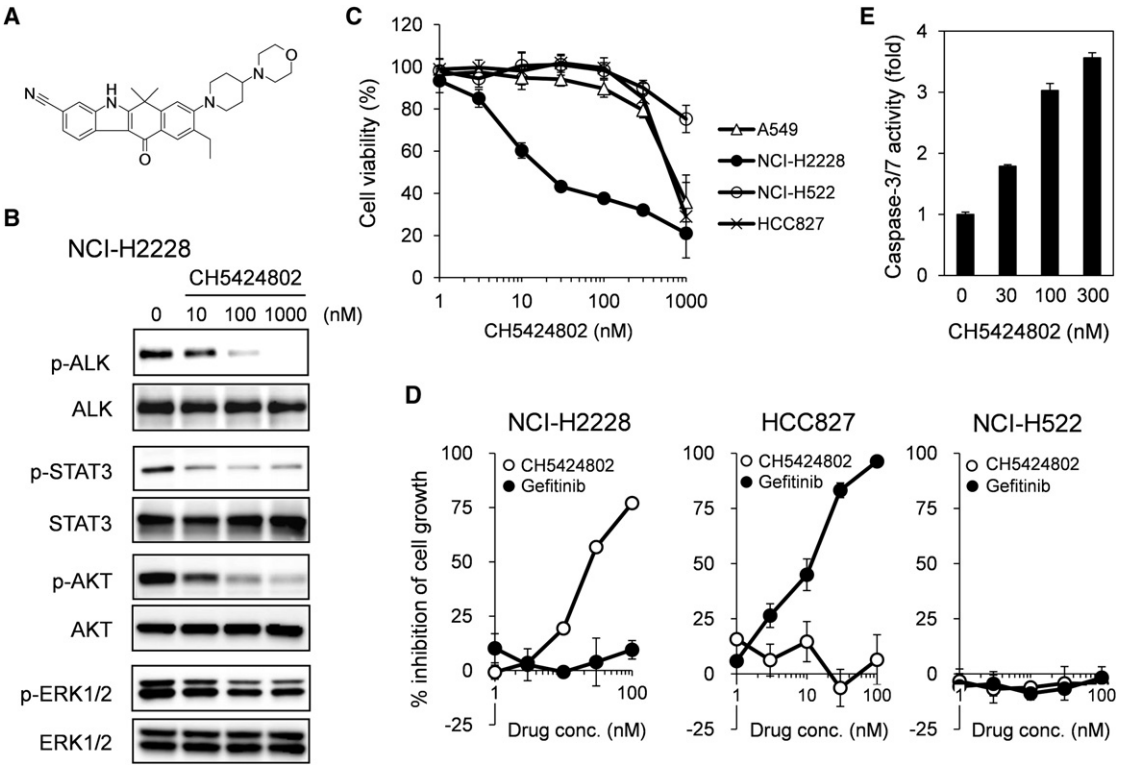

Figure 1. Selective Antitumor Activity in ALK-Positive NSCLC Cell Lines

(A) Chemical structure of CH5424802.

(B) Inhibition of ALK phosphorylation and signal transduction by CH5424802. NCI-H2228 cells were treated with CH5424802 for 2 hr at the indicated concentrations. ALK, STAT3, phosphorylated STAT3 (Tyr 705), AKT, phosphorylated AKT (Ser 473), ERK1/2, and phosphorylated ERK1/2 (Thr 202/Tyr 204) were detected by immunoblot analysis using antibodies to each of them. For phosphorylated ALK detection, cell lysates were immunoprecipitated with anti-phosphotyrosine antibody. The immunoprecipitants were then collected with Protein G Sepharose and subjected to immunoblot analysis using an anti-ALK antibody.

(C) Cells were seeded in a monolayer culture and incubated overnight, and then treated with various concentrations of CH5424802 for 5 days. The viable cells were measured by the CellTiter-Glo® Luminescent Cell Viability Assay. Data are shown as mean ± SD (n = 3).

(D) Cells were seeded on spheroid plates and incubated overnight, and then treated with CH5424802 or gefitinib for 5 days. The viable cells were measured by the CellTiter-Glo® Luminescent Cell Viability Assay. Data are shown as mean ± SD (n = 3). conc, concentration.

(E) Cells were seeded on spheroid plates and incubated overnight, and then treated with CH5424802 for 48 hr. Caspase 3/7 activation was measured by using Caspase-Glo3/7 assay kit. Data were calculated by dividing by the number of viable cells, and shown as mean ± SD (n = 3).

See also Figure S1 and Tables S1 and S2.

selective antitumor activity of CH5424802 against various cancer cells with genetic alterations of *ALK*.

We next tested the efficacy of CH5424802 using a mouse xenograft model. In the NCI-H2228 model, once-daily oral administration of CH5424802 resulted in dose-dependent tumor growth inhibition (ED_{50} = 0.46 mg/kg) and tumor regression (Figure 2A). Treatment of 20 mg/kg CH5424802 showed rapid tumor regression (168% tumor growth inhibition; $p < 0.001$), the tumor volume in any mouse was <30 mm^3 after 11 days of treatment (at day 28), a potent antitumor effect was maintained, and tumor regrowth did not occur throughout the 4-week drug-free period. In pharmacokinetic studies we determined the half-life (8.6 hr) and the oral bioavailability (70.8%) of CH5424802 in mice. At a repeated dose of 6 mg/kg, the mean plasma levels reached 1707, 1455, and 317 nM at 2, 7, and 24 hr post-dose, respectively. The plasma concentrations substantially exceed the in vitro IC_{50} values for NCI-H2228 (Figures 1C and 1D). At any dose level, no differences in body weight or gross signs of toxicity were observed between control- and CH5424802-treated mice. In contrast, CH5424802 had practically no antitumor effect in the xenograft model of A549, an NSCLC cell line that does not express ALK fusions (Figure 2A). Immunohistochemical assays demonstrated that the levels of phosphorylated ALK are decreased in the xenograft tumors harboring EML4-ALK after a single dose of CH5424802 (Figure 2B). In order to evaluate maximum efficacy, we conducted an efficacy study at 60 mg/kg against larger tumors (from an average tumor size of 340–350 mm^3) during long-term observation because the exposure of CH5424802 in mice had nearly peaked at 60 mg/kg. After administration of CH5424802 at 60 mg/kg for 3 weeks, tumor regrowth did not occur for 4 weeks (Figure 2C). There was no body weight loss, no significant changes in peripheral white blood cell and red blood cell counts, no elevations of aspartate aminotransferase (AST) and alanine aminotransferase (ALT), and no substantial changes in electrolytes (Na, K, and Cl) in mice at dose levels up to 60 mg/kg (Table S4). Similar

Table 1. Enzyme Inhibitory Activity of CH5424802 on Various Kinases

Tyr Kinase	IC_{50} (nM)	Ser/Thr Kinase	IC_{50} (nM)
ALK	1.9	AKT1	>5000
ALK F1174L	1.0	AKT2	>5000
ALK R1275Q	3.5	AKT3	>5000
INSR	550	Aurora A	>5000
KDR	1400	CDK1	>5000
ABL	>5000	CDK2	>5000
EGFR	>5000	MEK1	>5000
FGFR2	>5000	PKA	>5000
HER2	>5000	PKCα	>5000
IGF1R	>5000	PKCβ1	>5000
JAK1	>5000	PKCβ2	>5000
KIT	>5000	Raf-1	>5000
MET	>5000		
PDGFRβ	>5000		
SRC	>5000		

The in vitro kinase inhibitory assays in the presence of CH5424802 were carried out according to the Experimental Procedures. See also Table S1.

experiments were performed in models generated by implantation of KARPAS-299 ALCL cells and NB-1 neuroblastoma cells. In both the models, administration of CH5424802 led to tumor growth inhibition and tumor regression (Figure 2D). Tumor growth inhibition at 20 mg/kg was 119% for KARPAS-299 and 104% for NB-1 on day 20. Thus, CH5424802 has a potent therapeutic efficacy against tumors with genetic alterations of ALK in vivo.

To clarify the downstream signal pathway of EML4-ALK in NSCLC, we performed Affymetrix GeneChip analysis using CH5424802-treated NCI-H2228 xenograft tumors and comprehensively characterized the gene expression regulated by inhibition of activated ALK. The majority of genes commonly downregulated by treatment with CH5424802 were regulated by STAT3 (Table 2). There was not much difference between 4 and 20 mg/kg on genes downregulated by CH5424802. To validate the microarray data, we conducted real-time quantitative polymerase chain reaction (PCR) and confirmed a significant decrease in the expression of STAT3 target genes, such as *BCL3*, *NNMT*, *SOCS3*, and *BCL2L1*, in CH5424802-treated NCI-H2228 xenograft tumors (Figure 3A). Consistent with these results, CH5424802 suppressed the phosphorylation of STAT3 in a dose-dependent manner (2–20 mg/kg) (Figure 3B). A partial decrease in AKT phosphorylation was also observed in CH5424802-treated xenograft tumors.

Previous reports have demonstrated that STAT3 is required for ALK-mediated lymphomagenesis in ALCL (Chiarle et al., 2005). In the ALK-positive ALCL cell line KARPAS-299, we confirmed that CH5424802 completely inhibited the phosphorylation of STAT3 at Tyr705 (Figure S2A). Furthermore, the single knockdown of *STAT3* as well as *ALK* by siRNA led to a significant inhibition in cell growth (Figure S2B), suggesting that the STAT3 pathway would be critical for NPM-ALK signaling in ALCL. In contrast the growth of NCI-H2228 NSCLC cells expressing EML4-ALK was not affected by treatment of *STAT3* siRNA (Figure S2C). STAT3 activation is mediated through the Janus family kinases (JAK), which include four family members: JAK1, JAK2, JAK3, and TYK2 (Leonard and O'Shea, 1998). We also investigated the involvement of JAK1 and TYK2, upstream of STAT3 in NCI-H2228 cell growth, because NCI-H2228 cells do not express the other molecules, i.e., JAK2 and JAK3. However, single knockdown of either *JAK1* or *TYK1* did not cause a significant change in the cell viability of NCI-H2228, and similar results were observed in single knockdowns of *AKT1*, *ERK1*, and *ERK2* (Figure S2C).

Potency of CH5424802 against the L1196M Gatekeeper Mutation of ALK

The point mutations in the kinase domain are known as one of the mechanisms of acquired resistance to small-molecule kinase inhibitors. In particular the gatekeeper mutations, such as T790M in EGFR and T351I in ABL, are one of the most frequent causes of resistance. The sequence analysis of the gatekeeper region in the kinase domain revealed that L1196 of ALK corresponded to the gatekeeper residue (Figure 4A). A recent study using the gatekeeper mutant of NPM-ALK by a single nucleotide change showed that only L1196M, involving a substitution of methionine for leucine at position 1196 in ALK, exhibited increased kinase activity as compared with wild-type ALK (Lu et al., 2009). In contrast the substitution of arginine, proline, glutamine, or valine presented nondetectable or weaker kinase activity in cells. To evaluate the inhibitory effect of CH5424802 on the most predictable resistant mutation L1196M of ALK, we calculated the inhibitor constant (K_i) of CH5424802 or PF-02341066 using recombinant glutathione S-transferase (GST)-fused ALK and the mutant L1196M protein. CH5424802 had substantial inhibitory potency against both native ALK (K_i = 0.83 nM) and L1196M (K_i = 1.56 nM). In contrast the affinity of PF-02341066 for L1196M was found to be more than 10-fold weaker than that for the wild-type (Figures 4B; Figure S3A). To explore the effect of L1196M-driven cell growth on both compounds, we generated multiple stable transformants of Ba/F3 cells expressing EML4-ALK (variant 1) and the mutant L1196M (Figure 4C). CH5424802 showed a higher sensitivity against both native EML4-ALK and EML4-ALK L1196M-driven Ba/F3 cell clones grown in the absence of IL-3, as compared with the IL-3-dependent, EML4-ALK-independent Ba/F3 parental cells (Figures 4D; Figure S3B). Moreover, the sensitivities of L1196M-driven Ba/F3 cell clones to PF-02341066 were lower, closely resembling that of the Ba/F3 parental cells. The therapeutic indexes of CH5424802 and PF-02341066, the IC_{50} ratio of EML4-ALK L1196M-driven cell clones to the parental cells, were 7- to 12-fold and 1- to 2-fold. To confirm target inhibition of CH5424802 in each cell line, we tested the effect of CH5424802 on the phosphorylation of EML4-ALK. Consistent with the results of cell growth inhibition, CH5424802 could block cellular phosphorylation of ALK against both native EML4-ALK and the L1196M mutant in a concentration-dependent manner (Figure 4E).

The *EML4-ALK* C1156Y and L1196M mutations were recently identified in a pleural-effusion specimen from a patient with NSCLC who relapsed after a partial response to PF-02341066 (Choi et al., 2010). Therefore, we examined the inhibition of ALK C1156Y both in the cell-free ALK enzyme assay with

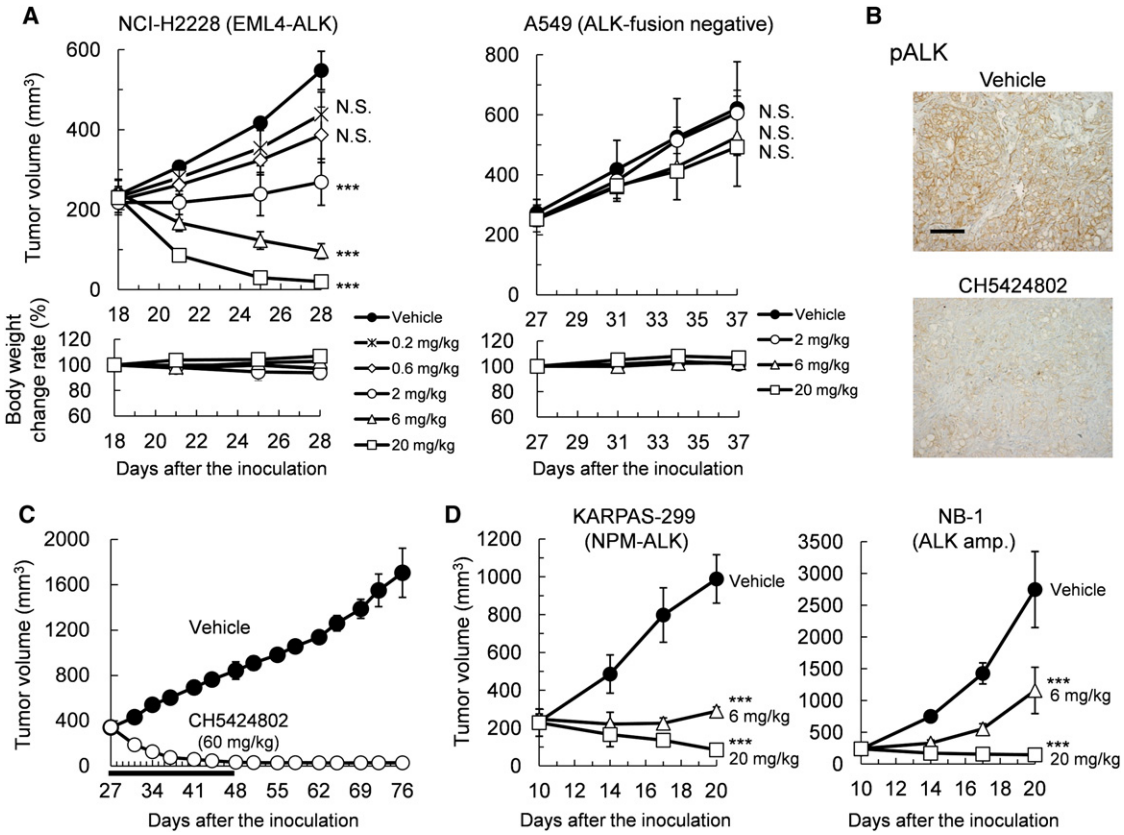

Figure 2. Antitumor Activity of CH5424802 in Mouse Xenograft Model of NSCLC

(A) Mice bearing NCI-H2228 and A549 were administered CH5424802 orally once daily for 11 days (NCI-H2228, days 18–28; A549, days 27–37) at the indicated doses. Tumor volume and body weight change for each dose group were measured. Data are shown as mean ± SD (n = 4–5). Parametric Dunnett's test: ***p < 0.001; N.S., not significant, versus vehicle treatment at final day.

(B) Mice bearing NCI-H2228 cells were orally administered a single dose of 0 (vehicle) or 20 mg/kg of CH5424802, and xenograft tumors were extracted at 4 hr post-dosing, fixed in formalin, and embedded in paraffin. Treated samples were immunostained for phospho-ALK (Tyr 1604). Scale bar, 100 μm.

(C) Mice bearing NCI-H2228 cells were administered CH5424802 orally once daily at 60 mg/kg for 3 weeks (days 27–47). Then tumor volume (mean ± SD) was continuously measured during the treatment and drug-free period for 4 weeks. Data are shown as mean ± SD (n = 5).

(D) Mice bearing KARPAS-299 and NB-1 were administered CH5424802 orally once daily for 11 days (days 10–20) at the indicated doses. Tumor volume for each dose group was measured. Data are shown as mean ± SD (n = 4–5). Parametric Dunnett's test: ***p < 0.001, versus vehicle treatment at final day.

See also Table S4.

GST-ALK C1156Y and a cell proliferation assay with Ba/F3 expressing EML4-ALK C1156Y. The in vitro enzyme inhibitory activity of CH5424802 to C1156Y was similar to that to wild-type ALK, whereas PF-02341066 showed slightly weaker inhibition (Figure S3A). Consistently, CH5424802 was effective against C1156Y-driven Ba/F3 cells, and the parent/EML4-ALK C1156Y IC_{50} ratio of CH5424802 was higher than that of PF-02341066 (20- to 33-fold versus 3- to 5-fold) (Figure S3B, lower panel). In addition to L1196M and C1156Y, F1174L mutation was identified as one of the causes of PF-02341066 resistance in a patient with an IMT harboring an *RANBP2-ALK* translocation who had progression while on PF-02341066 (Sasaki et al., 2010). We confirmed the inhibitory potency of CH5424802 to F1174L in both a cell-free kinase assay and an antiproliferative assay using the neuroblastoma KELLY cell line that expresses F1174L (Table S2). The inhibitory activity in vitro to F1174L (IC_{50} = 1.0 nM) was comparable to that to wild-type ALK (Table 1).

To further assess the in vivo antitumor activity of CH5424802 against L1196M-driven tumors, we used xenograft models of Ba/F3 expressing native EML4-ALK (clone #10) and the mutant L1196M (clone #303). We showed that administration of CH5424802 led to significant tumor regression against both native EML4-ALK- and L1196M-driven tumors (Figure 5). On the other hand, PF-02341066 (100 mg/kg) resulted in no significant tumor growth inhibition against L1196M-driven tumors. Furthermore, we confirmed that phospho-STAT3, one of the downstream targets of ALK, was abolished in both tumors that were treated with CH5424802 (Figure 5).

In recent studies, X-ray crystal structures of the ALK catalytic domain have been determined in the apo, ADP-, and kinase inhibitor-bound forms (Lee et al., 2010; Bossi et al., 2010). To understand the binding mode of CH5424802 with the ALK protein, we also determined the crystal structure of the human ALK and CH5424802 complex, and confirmed that CH5424802 binds to the ATP site of ALK in the DFG-in

Table 2. Downregulated Differentially Expressed Genes in CH5424802-Treated NCI-H2228 Xenograft Tumors

Probe ID	Gene	Mean Fold Change (versus vehicle) 4 mg/kg	20 mg/kg	Reported STAT3 Regulation	Reference
222088_s_at	*SLC2A3*	0.21	0.19	+	Dauer et al. (2005)
204908_s_at	*BCL3*	0.24	0.19	+	Dauer et al. (2005)
206697_s_at	*HP*	0.29	0.31	+	Zauberman et al. (2001)
209122_at	*ADFP*	0.30	0.23	–	–
202498_s_at	*SLC2A3*	0.32	0.32	+	Dauer et al. (2005)
208470_s_at	*HP*	0.33	0.33	+	Zauberman et al. (2001)
202237_at	*NNMT*	0.35	0.20	+	Tomida et al. (2008)
202912_at	*ADM*	0.39	0.43	+	Dauer et al. (2005)
211906_s_at	*SERPINB4*	0.39	0.32	+	Dauer et al. (2005)
201170_s_at	*BHLHB2*	0.41	0.22	–	–

Mice bearing NCI-H2228 cells were orally administered a dose of 0 (vehicle), 4, or 20 mg/kg of CH5424802, and the tumors were collected and lysed at 6 hr post-dose. Total RNA was extracted from xenograft tumors. Mean fold changes of duplicates identified by microarray compared to vehicle treatment are shown. Significantly ($p < 0.05$) common downregulated genes in both 4 and 20 mg/kg CH5424802-treated xenograft tumors were selected, and the top ten in 4 mg/kg are listed.

mode (Figures 6A and 6B). Carbonyl oxygen on the 11 position of the benzo[*b*]carbazole moiety of CH5424802 forms a crucial hydrogen bond with the backbone NH of Met1199 in the hinge region. Moreover, other hydrogen bonds are also formed with the NH group on 5 position and the cyano group on 3 position, which are embedded in a hydrogen-bonding network via the solute ethylene glycol and/or water molecules, to the neighboring amino acids Lys1150, Glu1167, Gly1269, Glu1270, and Arg1253 (Figure 6C). Another remarkable feature found in the CH5424802-ALK complex is a hydrophobic interaction, such as the CH/π hydrogen bond. The benzo[*b*]carbazole moiety of CH5424802 is positioned in the flat pocket (ATP-binding site) between the N- and C-lobes, of which the amino acid residues are hydrophobic. Leu1196 in N-lobe is close to the carbon atom of cyano group, and the distance between them is 3.57 Å, indicating an efficient CH/π interaction. However, no productive interaction was noted between PF-02341066 and Leu1196 (Figure 6D). An in silico modeling study suggested that CH5424802 could maintain the hydrogen-bonding network around cyano group; furthermore, the carbon atom of the cyano group could have a CH/π interaction with the CG atom-of the Met1196 instead of Leu1196 even in the L1196M-mutated model based on the crystal structures (data not

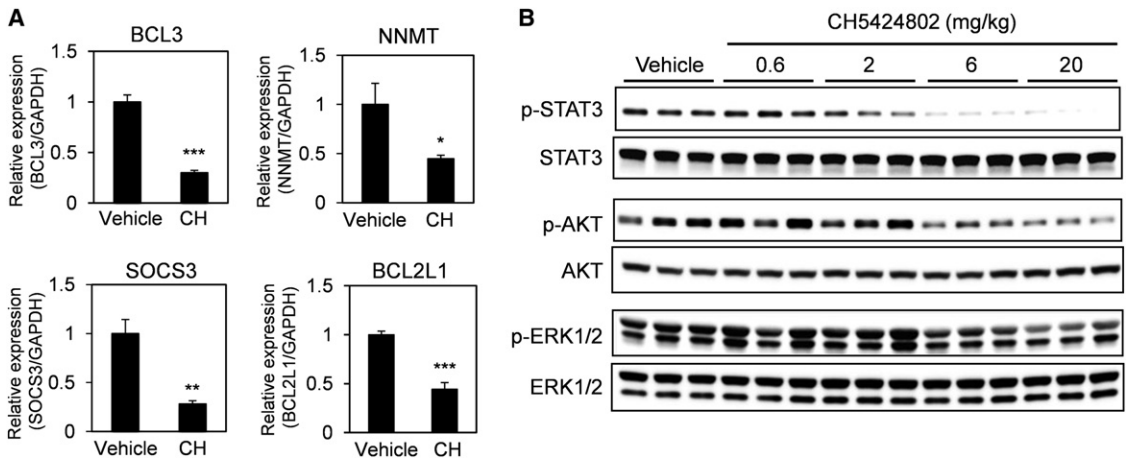

Figure 3. Downstream Signaling Pathway in NCI-H2228 Cells Harboring EML4-ALK

(A) Mice bearing NCI-H2228 cells were orally administered CH5424802 at 6 mg/kg, and the tumors were collected and lysed at 6 hr post-dosing. The levels of each transcript were measured by quantitative RT-PCR. Data are shown as mean ± SD (n = 3). Student's t test: *$p < 0.05$, **$p < 0.01$, ***$p < 0.001$, versus vehicle treatment.

(B) Mice bearing NCI-H2228 cells were orally administered CH5424802 at 0, 0.6, 2, 6, or 20 mg/kg, and the tumors were collected and lysed at 4 hr post-dosing. STAT3, phosphorylated STAT3 (Tyr 705), AKT, phosphorylated AKT (Ser 473), ERK1/2, and phosphorylated ERK1/2 (Thr 202/Tyr 204) were detected by immunoblot analysis using antibodies against each of them.

See also Figure S2.

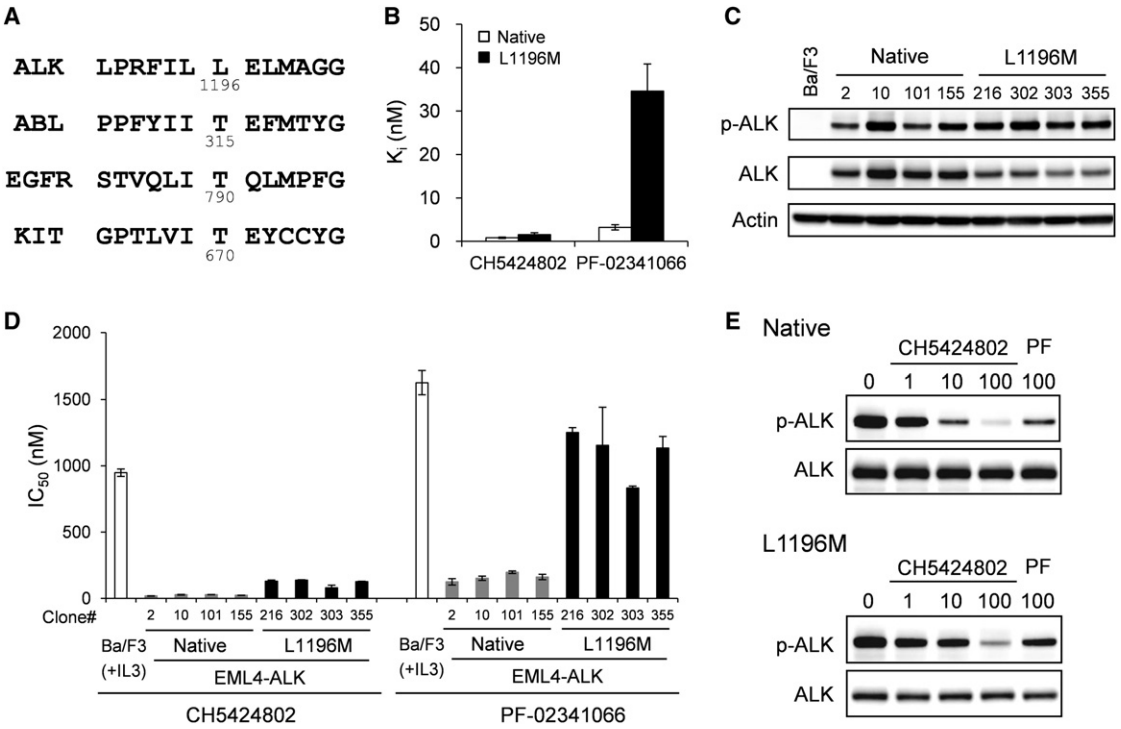

Figure 4. Blockade of CH5424802 against the L1196M Gatekeeper Mutation of ALK

(A) Alignment of sequences around the gatekeeper regions of ALK and other protein tyrosine kinases. The amino acid sequences around the gatekeeper region of ALK, ABL, EGFR, and KIT were compared.

(B) In vitro kinase inhibitory assays of ALK (amino acids 1081–1410) or the L1196M mutant fused to GST in the presence of CH5424802 or PF-02341066 were carried out. The K_i values were determined graphically from Dixon plots. Data are shown as geometric mean ± SD of three independent experiments.

(C) Ba/F3 cells were stably transfected with pcDNA3.1/hygro-EML4-ALK and the L1196M mutant. The expressions of p-ALK, ALK, and actin in each clone were detected by immunoblot analysis.

(D) Ba/F3 cells grown in the presence of IL-3, or Ba/F3 cells expressing native *EML4-ALK* (clone #2, #10, #101, and #155) and *EML4-ALK L1196M* (clone #216, #302, #303, and #355), were treated with CH5424802 or PF-02341066 for 48 hr, and then the viable cells were measured by the CellTiter-Glo® Luminescent Cell Viability Assay. IC_{50} values were determined by plotting the drug concentration versus percentage of cell growth inhibition. Data are shown as mean ± SD (n = 3).

(E) Ba/F3 cells, expressing native EML4-ALK (clone #10) and EML4-ALK L1196M (clone #303), were treated with the indicated concentrations of CH5424802 or 100 nM PF-02341066 for 2 hr. The levels of ALK and phosphor-ALK (Tyr 1604) were detected by immunoblot analysis using antibodies against each of them.

See also Figure S3.

shown). These data support the higher sustainability of CH5424802 against L1196M mutation as confirmed by biological assay (Figure 4B).

DISCUSSION

CH5424802 (development code: AF802) is currently being investigated in phase I/II clinical trials for patients with ALK-positive NSCLC (JAPIC ID JapicCTI-101264). A remarkable characteristic of CH5424802 is the high selectivity for ALK among various types of kinases, including c-MET and INSR. Kinase selectivity of a compound is related to the number of hinge hydrogen bonds with the kinase inhibitor. Most of the approved kinase inhibitors, such as erlotinib, imatinib, and lapatinib, form only one hydrogen bond with the hinge region (Ghose et al., 2008). Crystal structural analysis revealed that CH5424802 has one hinge hydrogen bond with the backbone of NH of Met1199 (Figure 6C), whereas other ALK inhibitors, PF-02341066, NVP-TAE684, and PHA-E429, form two or three hinge hydrogen bonds (PDB IDs 2XP2, 2XB7, and 2XBA), suggesting that our benzo[*b*]carbazole derivative may be beneficial in achieving higher selectivity for ALK.

A c-MET/ALK inhibitor PF-02341066 is effective against advanced NSCLC carrying activated ALK (Kwak et al., 2010). The grade 3 or 4 adverse events for PF-02341066 in clinical development consist mostly of ALT and AST elevations (6% each); however, to our knowledge, the precise mechanism remains unknown. NVP-TAE684 suppresses cellular proliferation of an NPM-ALK fusion kinase-dependent cell line (Galkin et al., 2007). Although the IC_{50} of INSR was 10–20 nM in an in vitro enzyme assay, this was not consistent with cellular INSR activity in H-4-II-E rat hepatoma cells. Also, NVP-TAE684 is preferentially efficacious to not only ALK-dependent cell lines but also the neuroblastoma cell lines without obvious ALK gene alterations, implicating IGF-IR as a potential target (McDermott et al., 2008). Furthermore, the chronic inhibition of IGF-1R/INSR results in sustained hyperinsulinemia in mice using another ALK inhibitor, GSK1838705A (Sabbatini et al., 2009). Because *ALK* expression in normal adult tissues is limited to very low levels, selective ALK inhibitors would exhibit sufficiently wide

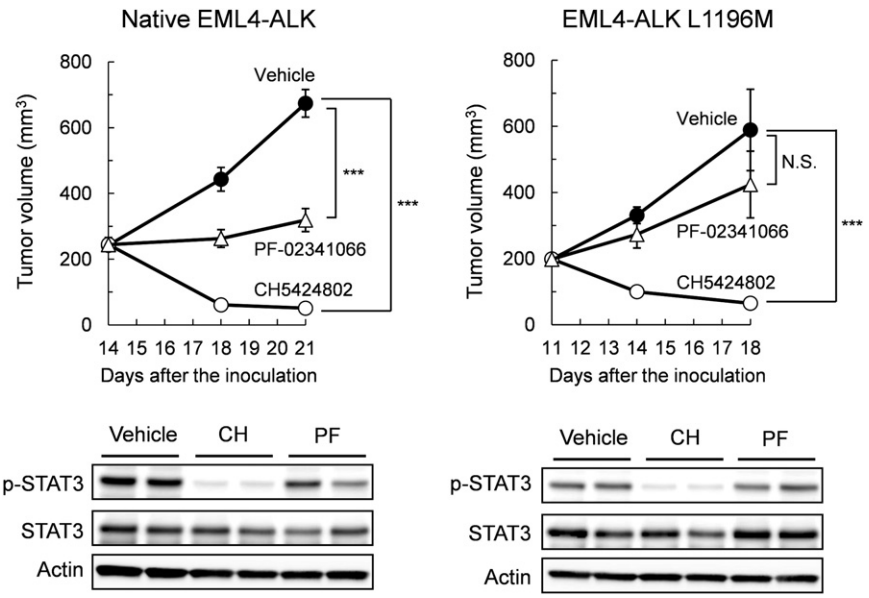

Figure 5. Efficacy in Mice Models of Native EML4-ALK and EML4-ALK L1196M-Driven Tumors

Mice bearing Ba/F3-EML4-ALK (clone #10) and EML4-ALK L1196M (clone #303) were administered vehicle, CH5424802 (60 mg/kg), or PF-02341066 (100 mg/kg) orally once daily for 8 days. Tumor volume for each dose group was measured. Data are shown as mean ± SD (n = 5). Parametric Dunnett's test: ***$p < 0.001$; N.S., not significant, versus vehicle treatment at final day. For pharmacodynamic assay, mice bearing Ba/F3-EML4-ALK (clone #10) and -EML4-ALK L1196M (clone #303) were orally administered at single dose of vehicle, CH5424802 (60 mg/kg), or PF-02341066 (100 mg/kg), and the tumors were collected and lysed at 4 hr post-dosing. STAT3 and phosphorylated STAT3 (Tyr 705) were detected by immunoblot analysis using antibodies against each of them (n = 2 per group).

therapeutic windows in patients with ALK-activated cancers. We expect that CH5424802 with ALK selectivity could provide a higher exposure than that of the efficacious dose, leading to greater efficacy in clinic.

CH5424802 showed a potent efficacy against ALK-addicted tumors, such as NSCLC expressing *EML4-ALK*, ALCL expressing *NPM-ALK*, and *ALK*-amplified neuroblastoma, in vitro and in vivo. Furthermore, we found that CH5424802 could induce caspase-3/7 activation in spheroids with in vitro 3D tissue structure that mimics in vivo tumors (Figure 1E), suggesting that the ability to induce apoptosis by ALK inhibition might be reflected in strong tumor regression. We examined the change in the gene expression or signal transduction of xenografted tumors expressing EML4-ALK protein and confirmed the suppression of the STAT3 pathway following treatment with CH5424802. The STAT3 target genes, such as *BCL3* and *NNMT*, as well as phospho-ALK and -STAT3 might be useful pharmacodynamic markers for the clinical evaluation of ALK inhibitors. However,

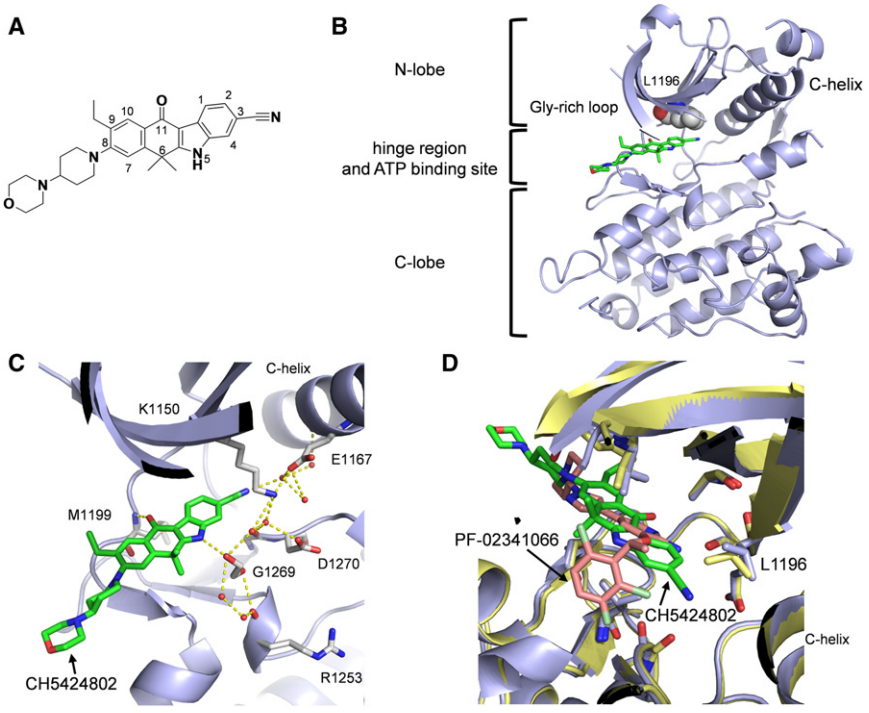

Figure 6. X-ray Structure of the ALK and CH5424802 Complex

(A) Chemical structure of CH5424802. The positions of substituents are numbered.

(B) Overall structure of ALK containing CH5424802 shown as a cartoon diagram in light blue (PDB ID 3AOX). CH5424802 is shown as a stick model, colored by element type (C in green, O in red, and N in blue). L1196 residue is shown as a space-filling model, colored by element type as the ligand except C in white.

(C) Interaction of CH5424802 with ALK at the ATP-binding site. Solvent water molecules forming a hydrogen-bonding network with the ligand are depicted within red small spheres. An ethylene glycol (cryosolvent) and amino acid residues, which form hydrogen bonds to the ligand directly or via water molecules, are depicted as stick models colored in the same manner as (B).

(D) Superposition of CH5424802-hALK and PF-02341066-hALK (PDB ID 2XP2). The superposition was based on the Cα positions of the two complexes. Protein cartoon diagrams of CH5424802 complex are in light blue, and PF-02341066 is in pale yellow. PF-02341066 molecule as a stick model (C in pink) is overlaid on CH5424802. In each complex, L1196 is shown as a stick model.

See also Table S5.

to our knowledge, the full downstream targets of EML4-ALK in NSCLC cells remain unknown. The growth of NCI-H2228 NSCLC cells expressing EML4-ALK was not affected in the single knockdown of gene including STAT3 (Figure S2C), although the STAT3 pathway is critical for the growth of ALCL cells expressing NPM-ALK (Figure S2B) (Chiarle et al., 2005). A recent report showed that overexpression of *EML4-ALK* variant 3 in 293T cells resulted in increased phosphorylation of STAT3, AKT, and ERK1/2, whereas enhanced phosphorylation of ERK1/2 was not prominent in COS-7 cells (Wong et al., 2011). In our studies treatment of CH5424802 in NCI-H2228 led to the reduction of both phospho-STAT3 and phospho-AKT (Figure 1B). Unlike proliferation of *NPM-ALK*-positive cells, that of *EML4-ALK*-positive cells might require combined multiple downstream signaling pathways, but not a single pathway. The subcellular localization of ALK fusion proteins likely depends on the fusion partner. NPM-ALK in ALCL is present in both the nucleus and cytoplasm, whereas EML4-ALK in NSCLC has been detected in the cytoplasm, but not in the nucleus (Takeuchi et al., 2009). From these observations the downstream pathway of ALK appears to depend on the fusion partners and cell types. Further detailed studies are needed to elucidate the downstream signal of EML4-ALK in NSCLC to explore options for combination therapy based on clinical rationale.

In order to verify the potency to combat resistance to ALK inhibitors, we first focused on the gatekeeper mutation because it is one of the most frequently reported mutants commonly occurring in clinical kinase inhibitor resistance and is located next to the ATP-binding region. Gatekeeper mutations in *EGFR*, *ABL*, or *KIT* are involved in the resistance to certain kinase inhibitors used clinically (Branford et al., 2002; Pao et al., 2005; Tamborini et al., 2004). In this study we confirmed that CH5424802 displayed substantial efficacy against gatekeeper mutant L1196M-driven tumors in vivo, despite a slightly weaker affinity of CH5424802 for L1196M as compared to native ALK. In the in vitro experiments using Ba/F3 expressing EML4-ALK or the mutant L1196M, the IC_{50} ratio of CH5424802 in L1196M (7- to 12-fold) was similar to that of PF-02341066 in native EML4-ALK (8- to 13-fold) (Figure S3B), which is clinically effective. The efficacy of CH5424802 would be insusceptible to differences in subtle affinity caused by single amino acid changes such as L1196M, compared with that of PF-02341066, because CH5424802 has a higher IC_{50} ratio in Ba/F3 expressing native EML4-ALK than PF-02341066 (33- to 52-fold versus 8- to 13-fold) (Figure S3B). On the other hand, in L1196M-driven Ba/F3 cells, the IC_{50} ratio of PF-02341066 was 1- to 2-fold, and consistently, L1196M-driven Ba/F3 tumors showed resistance to PF-02341066 (100 mg/kg qd) in vivo (Figure 5). In clinical pharmacokinetics of PF-02341066 (250 mg bid) at MTD/RP2D, the median trough plasma concentration at steady state was 274 ng/ml (Tan et al., 2010, J. Clin. Oncol., abstract), and at this exposure level, PF-02341066 was effective against *ALK*-positive NSCLC. In our experiments after repeated qd dosing of 100 mg/kg PF-02341066 in mice, the mean plasma levels reached 2800, 989, and 899 ng/ml at 2, 7, and 24 hr, respectively, and thus, a sufficiently higher exposure was achieved in mice than by the clinical dose.

In a previous study an irreversible EGFR kinase inhibitor, such as neratinib (HKI-272), provided the ability to inhibit gatekeeper mutations of EGFR; however, the clinical efficacy of these inhibitors has been limited (Sequist et al., 2010). This clinical result would be due to toxicities of neratinib associated with wild-type EGFR inhibition, such as diarrhea and rash, demonstrating the need for mutant-selective kinase inhibitors (Zhou et al., 2009). On the other hand, in the case of ALK inhibitors, the effect of on-target toxicity by inhibition of wild-type ALK would be less because *ALK* expression in normal tissues is restricted, and *ALK*-deficient mice revealed no obvious abnormalities in any tissue (Bilsland et al., 2008), and in clinical trial of PF-02341066, on-target toxicity of ALK has not been clarified yet. Additionally, in the case of potent BCR-ABL inhibitor dasatinib, although E255K, L248V, and G250E in BCR-ABL were 4.45- to 5.61-fold less sensitive to dasatinib than the wild-type in a BCR-ABL-transfected Ba/F3 cell system (Redaelli et al., 2009), a favorable response rate was achieved in patients with these imatinib-resistant mutations in clinic (Müller et al., 2009). A key determinant of clinical efficacy to drug would depend on the therapeutic window between efficacy and safety.

The difference in sensitivity to the compound between native ALK and the mutant L1196M in Ba/F3 cells was slightly greater than that in a cell-free enzyme assay. For native ALK and ALK 1196M, the K_M values for ATP were 34 and 25 μM, respectively, in our kinase assay. The difference in this ATP affinity might be slightly reflected in the sensitivity in Ba/F3 cells.

We expect that CH5424802 might provide therapeutic opportunities for patients with acquired resistance to PF-02340166. In order to elucidate alternative acquired resistant mechanisms (e.g., amplification of other oncogenes), further genetic analyses are needed for the patients with resistance to ALK inhibitors.

EXPERIMENTAL PROCEDURES

Compounds and Cell Lines

CH5424802, 9-ethyl-6,6-dimethyl-8-[4-(morpholin-4-yl)piperidin-1-yl]-11-oxo-6,11-dihydro-5*H*-benzo [*b*]carbazole-3-carbonitrile hydrochloride, was synthesized at Chugai Pharmaceutical Co., Ltd., according to the procedure described in WO2010143664. PF-02341066 was purchased from Selleck Chemicals or synthesized according to the procedure described in WO2006021884. Cell lines were obtained from American Type Culture Collection (ATCC) or RIKEN. Each cell line was cultured using the medium recommended by the suppliers.

Kinase Inhibitory Assays In Vitro

Protein kinases were purchased from Carna Biosciences or Millipore Corporation. The inhibitory ability against each kinase except for MEK1 and Raf-1 was evaluated by examining their ability to phosphorylate various substrate peptides in the presence of CH5424802 using time-resolved fluorescence resonance energy transfer (TR-FRET) assay or fluorescence polarization (FP) assay (details of assay conditions for each kinase are available in Table S1). The inhibitory activity against MEK1 was evaluated by quantitative analysis of the phosphorylation of a substrate peptide by a recombinant ERK2 protein in the presence of CH5424802. The inhibitory activity against Raf-1 was evaluated by examining the ability of the kinases to phosphorylate MEK1 in the presence of CH5424802.

Immunoblotting and Immunoprecipitation

Cells were lysed in Cell Lysis Buffer (Cell Signaling Technology) containing 1 mM PMSF, 1% (v/v) phosphate inhibitor cocktail 1, 1% (v/v) phosphate inhibitor cocktail 2, and Complete Mini, EDTA-Free 1 (Roche). Cell lysates were subjected to sodium dodecyl sulfate-polyacrylamide gel electrophoresis (SDS-PAGE), and the separated proteins were electrophoretically transferred to Immobilon-P membranes (Millipore). After blocking in Blocking One (Nacalai

Tesque, Inc.), the membranes were incubated independently in the primary antibodies diluted with anti-ALK (Invitrogen; #51-3900), anti-STAT3, anti-Phospho-STAT3 (Tyr 705), anti-AKT, anti-Phospho-AKT (Ser 473), anti-p44/42 MAP Kinase (ERK1/2), anti-Phospho-ERK1/2 (Thr 202/Tyr 204), anti-ALK (C26G7), anti-Phospho-ALK (Tyr 1604) (Cell Signaling Technology; #3341), and anti-actin (Sigma). For the detection of phosphorylated ALK in NCI-H2228 cells, cell lysates were immunoprecipitated with anti-phosphotyrosine (PY-20) antibody (BD Biosciences). The immunoprecipitants were then collected with Protein G Sepharose (GE Healthcare) and subjected to immunoblot analysis using an anti-ALK antibody. The membranes were incubated with an anti-rabbit or anti-mouse IgG, HRP-linked antibody (Cell Signaling Technology). The bands were detected with ECL Plus (GE Healthcare) followed by LAS-4000 (Fujifilm).

Cell Growth Inhibition and Caspase-3/7 Assay

Cells were cultured in 96-well plates overnight and incubated with various concentrations of compound for the indicated time. For spheroid cell growth inhibition assay, cells were seeded on spheroid plates (Sumilon Celltight Spheroid 96U; Sumitomo Bakelite Inc.), incubated overnight, and then treated with compound for the indicated times. The viable cells were measured by the CellTiter-Glo® Luminescent Cell Viability Assay (Promega). Caspase-3/7 assay was evaluated using the Caspase-Glo 3/7 Assay Kit (Promega).

In Vivo Studies

Cell lines were used to evaluate the antitumor activity of CH5424802 in vivo. They were grown as s.c. tumors in SCID or nude mice (Charles River Laboratories). Therapeutic experiments were started (day 0) when the tumor reached ~250 or ~350 mm^3. Mice were randomized to treatment groups to receive vehicle or CH5424802 (oral, qd) for the indicated duration. Final concentration of vehicle was 0.02 N HCl, 10% DMSO, 10% Cremophor EL, 15% PEG400, and 15% HPCD (2-hydroxypropyl-β-cyclodextrin). The length (L) and width (W) of the tumor mass were measured, and the tumor volume (TV) was calculated as: $TV = (L \times W^2)/2$. Tumor growth inhibition was calculated using the following formula: tumor growth inhibition = $[1 - (T - T_0)/(C - C_0)] \times 100$, where T and T_0 are the mean tumor volumes on a specific experimental day and on the first day of treatment, respectively, for the experimental groups and likewise, where C and C_0 are the mean tumor volumes for the control group. The effective dose for 50% inhibition (ED_{50}) was calculated from the values of tumor growth inhibition on the final experimental day using XLfit version 5.1.0.0. The rate of change in body weight (BW) was calculated using the following formula: $BW = W/W_0 \times 100$, where W and W_0 are the body weights on a specific experimental day and on the first day of treatment, respectively. All animal experiments in this study were performed in accordance with protocols approved by the Institutional Animal Care and Use Committee (IACUC) of Chugai Pharmaceutical Co., Ltd.

Immunohistochemistry

Xenograft tumors were extracted, fixed in formalin, and embedded in paraffin. Immunostaining for phosphorylated ALK was performed using phospho-ALK (Tyr 1604) antibody (Cell Signaling Technology; #3341). Immunohistochemistry was performed using the DISCOVERY XT automated staining platform (Ventana Medical Systems).

Microarray and Quantitative RT-PCR

Total RNA was extracted using the RNeasy kit (QIAGEN), and reverse transcribed, labeled, and hybridized to Human Genome U133 Plus 2.0 arrays (Affymetrix) according to the manufacturer's instructions. The expression value for each probe was calculated using the GC-RMA algorithm. For quantitative RT-PCR, RNA was amplified in QuantiFast Multiplex RT-PCR (QIAGEN) using a Universal probe library (Roche Applied Science) and the LightCycler System (Roche). Glyceraldehyde-3-phosphate dehydrogenase (GAPDH) served as an internal control.

Generation of Recombinant ALK and the Mutant Proteins

To evaluate the in vitro kinase assay of ALK, we generated a GST-tagged, kinase domain (amino acid 1081–1410) of ALK or the mutants by using a Bac-to-Bac Baculovirus Expression System (Invitrogen) in Sf-9 insect cells according to the manufacturer's protocols. Mutant constructs were generated using the QuikChange Site-Directed Mutagenesis Kit (Stratagene). The cells were lysed in lysis buffer (phosphate-buffered saline with 0.1% Triton X-100 and Roche Complete protease inhibitors) and centrifuged. Glutathione Sepharose 4B (GE Healthcare) was incubated for 1 hr with the soluble fraction of the lysate and washed in buffer A (50 mM Tris-HCl [pH8.0], 150 mM NaCl, and 1% Triton X-100). The proteins were eluted with elution buffer (50 mM Tris-HCl [pH8.0], 150 mM NaCl, 0.5% Triton X-100, and 20 mM reduced L-glutathione). The protein expression and purification were confirmed by SDS-PAGE.

Stable Ba/F3 Transfectants

The *EML4-ALK* gene (variant 1) and the L1196M were inserted into pcDNA3.1/hygro vector (Invitrogen). EML4-ALK L1196M was generated using the QuikChange Site-Directed Mutagenesis Kit (Stratagene) and confirmed by resequencing the whole construct. Ba/F3-EML4-ALK and the L1196M cell lines were generated by transfecting Ba/F3 cells with pcDNA3.1/hygro-EML4-ALK and the L1196M mutant by using the NucleoFector device (Amaxa); stable transfectants were then isolated from the cultured medium without IL-3.

Crystallization and Structural Determination of ALK-CH5424802 Complex

Protein crystallography was performed by proteros biostructures GmbH (Martinsried/Munich, Germany). The kinase domain of human ALK (residues 1069–1411) was expressed in SF9 cells with a GST-fusion tag, which was removed by protease cleavage during purification; the kinase domain was then purified using affinity, size exclusion, and ion-exchange chromatography. The purified protein was concentrated to 20–40 mg/ml and stored at −80°C until use.

Crystals were obtained at 4°C from sitting drops using a reservoir solution (5%–20% PEG 550 MME and 0.1 M maleic acid [pH 5.5]) by vapor diffusion. The crystals were shock-frozen in liquid nitrogen after the addition of 22% ethyleneglycol. Diffraction data were collected at 90 K at beamline X06SA in SLS using a PILATUS 6M detector (DECTRIS Ltd.). The data set was processed with XDS and scaled with XSCALE (Kabsch, 1993) in the space group $P2_12_12_1$. The structure of the ALK and CH5424802 complex was determined by molecular replacement by Phaser (McCoy et al., 2007) with an insulin receptor kinase (PDB ID 1GAG). The crystals contain one monomer of ALK in the asymmetric unit. The model was rebuilt manually in Coot (Emsley et al., 2010), and refined with REFMAC5 (Murshudov et al., 1997) to a final resolution of 1.75 Å. B factors were refined isotropically. TLS refinement was used to improve maps and models. The final model consisted of residues 1086–1401 with three breaks (residues 1124–1127, 1137–1143, 1281–1287 were disordered). The resulting electron density revealed an unambiguous binding mode of CH5424802. For crystallographic data and refinement statistics, see Table S5.

ACCESSION NUMBERS

The atomic coordinates of the ALK-CH5424802 complex structure have been deposited in the RSCB Protein Data Bank under accession number 3AOX. The microarray data have been deposited in the GEO database (GEO number: GSE25118).

SUPPLEMENTAL INFORMATION

Supplemental Information includes Supplemental Experimental Procedures, three figures, and five tables and can be found with this article online at doi:10.1016/j.ccr.2011.04.004.

ACKNOWLEDGMENTS

We thank Y. Tachibana, M. Izawa, K. Sakata, T. Fujii, K. Kashima, Y. Sato, and T. Takahashi for pharmacological assays; K. Kinoshita, K. Aso, N. Furuichi, T. Ito, and H. Kawada for chemical synthesis; and S. Nagel, M. Moertl, and A. Jestel at proteros biostructures GmbH for protein crystallography of the ALK-ligand complex structures.

Received: November 9, 2010
Revised: February 23, 2011
Accepted: April 2, 2011
Published: May 16, 2011

REFERENCES

Bilsland, J.G., Wheeldon, A., Mead, A., Znamenskiy, P., Almond, S., Waters, K.A., Thakur, M., Beaumont, V., Bonnert, T.P., Heavens, R., et al. (2008). Behavioral and neurochemical alterations in mice deficient in anaplastic lymphoma kinase suggest therapeutic potential for psychiatric indications. Neuropsychopharmacology *33*, 685–700.

Bossi, R.T., Saccardo, M.B., Ardini, E., Menichincheri, M., Rusconi, L., Magnaghi, P., Orsini, P., Avanzi, N., Borgia, A.L., Nesi, M., et al. (2010). Crystal structures of anaplastic lymphoma kinase in complex with ATP competitive inhibitors. Biochemistry *49*, 6813–6825.

Branford, S., Rudzki, Z., Walsh, S., Grigg, A., Arthur, C., Taylor, K., Herrmann, R., Lynch, K.P., and Hughes, T.P. (2002). High frequency of point mutations clustered within the adenosine triphosphate-binding region of BCR/ABL in patients with chronic myeloid leukemia or Ph-positive acute lymphoblastic leukemia who develop imatinib (STI571) resistance. Blood *99*, 3472–3475.

Chen, Y., Takita, J., Choi, Y.L., Kato, M., Ohira, M., Sanada, M., Wang, L., Soda, M., Kikuchi, A., Igarashi, T., et al. (2008). Oncogenic mutations of ALK kinase in neuroblastoma. Nature *455*, 971–974.

Chiarle, R., Simmons, W.J., Cai, H., Dhall, G., Zamo, A., Raz, R., Karras, J.G., Levy, D.E., and Inghirami, G. (2005). Stat3 is required for ALK-mediated lymphomagenesis and provides a possible therapeutic target. Nat. Med. *11*, 623–629.

Choi, Y.L., Takeuchi, K., Soda, M., Inamura, K., Togashi, Y., Hatano, S., Enomoto, M., Hamada, T., Haruta, H., Watanabe, H., et al. (2008). Identification of novel isoforms of the EML4-ALK transforming gene in non-small cell lung cancer. Cancer Res. *68*, 4971–4976.

Choi, Y.L., Soda, M., Yamashita, Y., Ueno, T., Takashima, J., Nakajima, T., Yatabe, Y., Takeuchi, K., Hamada, T., Haruta, H., et al. (2010). EML4-ALK mutations in lung cancer that confer resistance to ALK inhibitors. N. Engl. J. Med. *363*, 1734–1739.

Christensen, J.G., Zou, H.Y., Arango, M.E., Li, Q., Lee, J.H., McDonnell, S.R., Yamazaki, S., Alton, G.R., Mroczkowski, B., and Los, G. (2007). Cytoreductive antitumor activity of PF-2341066, a novel inhibitor of anaplastic lymphoma kinase and c-Met, in experimental models of anaplastic large-cell lymphoma. Mol. Cancer Ther. *6*, 3314–3322.

Dauer, D.J., Ferraro, B., Song, L., Yu, B., Mora, L., Buettner, R., Enkemann, S., Jove, R., and Haura, E.B. (2005). Stat3 regulates genes common to both wound healing and cancer. Oncogene *24*, 3397–3408.

Emsley, P., Lohkamp, B., Scott, W.G., and Cowtan, K. (2010). Features and development of Coot. Acta Crystallogr. D Biol. Crystallogr. *66*, 486–501.

Galkin, A.V., Melnick, J.S., Kim, S., Hood, T.L., Li, N., Li, L., Xia, G., Steensma, R., Chopiuk, G., Jiang, J., et al. (2007). Identification of NVP-TAE684, a potent, selective, and efficacious inhibitor of NPM-ALK. Proc. Natl. Acad. Sci. USA *104*, 270–275.

George, R.E., Sanda, T., Hanna, M., Fröhling, S., Luther, W., Zhang, J., Ahn, Y., Zhou, W., London, W.B., McGrady, P., et al. (2008). Activating mutations in ALK provide a therapeutic target in neuroblastoma. Nature *455*, 975–978.

Ghose, A.K., Herbertz, T., Pippin, D.A., Salvino, J.M., and Mallamo, J.P. (2008). Knowledge based prediction of ligand binding modes and rational inhibitor design for kinase drug discovery. J. Med. Chem. *51*, 5149–5171.

Griffin, C.A., Hawkins, A.L., Dvorak, C., Henkle, C., Ellingham, T., and Perlman, E.J. (1999). Recurrent involvement of 2p23 in inflammatory myofibroblastic tumors. Cancer Res. *59*, 2776–2780.

Inamura, K., Takeuchi, K., Togashi, Y., Nomura, K., Ninomiya, H., Okui, M., Satoh, Y., Okumura, S., Nakagawa, K., Soda, M., et al. (2008). EML4-ALK fusion is linked to histological characteristics in a subset of lung cancers. J. Thorac. Oncol. *3*, 13–17.

Iwahara, T., Fujimoto, J., Wen, D., Cupples, R., Bucay, N., Arakawa, T., Mori, S., Ratzkin, B., and Yamamoto, T. (1997). Molecular characterization of ALK, a receptor tyrosine kinase expressed specifically in the nervous system. Oncogene *14*, 439–449.

Janoueix-Lerosey, I., Lequin, D., Brugières, L., Ribeiro, A., de Pontual, L., Combaret, V., Raynal, V., Puisieux, A., Schleiermacher, G., Pierron, G., et al. (2008). Somatic and germline activating mutations of the ALK kinase receptor in neuroblastoma. Nature *455*, 967–970.

Kabsch, W. (1993). Automatic processing of rotation diffraction data from crystals of initially unknown symmetry and cell constants. J. Appl. Crystallogr. *26*, 795–800.

Kwak, E.L., Bang, Y., Camidge, D.R., Shaw, A.T., Solomon, B., Maki, R.G., Ou, S.I., Dezube, B.J., Jänne, P.A., Costa, D.B., et al. (2010). Anaplastic lymphoma kinase inhibition in non–small-cell lung cancer. N. Engl. J. Med. *363*, 1693–1703.

Lee, C.C., Jia, Y., Li, N., Sun, X., Ng, K., Ambing, E., Gao, M.Y., Hua, S., Chen, C., Kim, S., et al. (2010). Crystal structure of the ALK (anaplastic lymphoma kinase) catalytic domain. Biochem. J. *430*, 425–437.

Leonard, W.J., and O'Shea, J.J. (1998). Jaks and STATs: biological implications. Annu. Rev. Immunol. *16*, 293–322.

Lu, L., Ghose, A.K., Quail, M.R., Albom, M.S., Durkin, J.T., Holskin, B.P., Angeles, T.S., Meyer, S.L., Ruggeri, B.A., and Cheng, M. (2009). ALK mutants in the kinase domain exhibit altered kinase activity and differential sensitivity to small molecule ALK inhibitors. Biochemistry *48*, 3600–3609.

McCoy, A.J., Grosse-Kunstleve, R.W., Adams, P.D., Winn, M.D., Storoni, L.C., and Read, R.J. (2007). Phaser crystallographic software. J. Appl. Crystallogr. *40*, 658–674.

McDermott, U., Iafrate, A.J., Gray, N.S., Shioda, T., Classon, M., Maheswaran, S., Zhou, W., Choi, H.G., Smith, S.L., Dowell, L., et al. (2008). Genomic alterations of anaplastic lymphoma kinase may sensitize tumors to anaplastic lymphoma kinase inhibitors. Cancer Res. *68*, 3389–3395.

Morris, S.W., Kirstein, M.N., Valentine, M.B., Dittmer, K.G., Shapiro, D.N., Saltman, D.L., and Look, A.T. (1994). Fusion of a kinase gene, ALK, to a nucleolar protein gene, NPM, in non-Hodgkin's lymphoma. Science *263*, 1281–1284.

Mossé, Y.P., Laudenslager, M., Longo, L., Cole, K.A., Wood, A., Attiyeh, E.F., Laquaglia, M.J., Sennett, R., Lynch, J.E., Perri, P., et al. (2008). Identification of ALK as a major familial neuroblastoma predisposition gene. Nature *455*, 930–935.

Müller, M.C., Cortes, J.E., Kim, D.W., Druker, B.J., Erben, P., Pasquini, R., Branford, S., Hughes, T.P., Radich, J.P., Ploughman, L., et al. (2009). Dasatinib treatment of chronic-phase chronic myeloid leukemia: analysis of responses according to preexisting BCR-ABL mutations. Blood *114*, 4944–4953.

Murshudov, G.N., Vagin, A.A., and Dodson, E.J. (1997). Refinement of macromolecular structures by the maximum-likelihood method. Acta Crystallogr. D Biol. Crystallogr. *53*, 240–255.

O'Hare, T., Shakespeare, W.C., Zhu, X., Eide, C.A., Rivera, V.M., Wang, F., Adrian, L.T., Zhou, T., Huang, W.S., Xu, Q., et al. (2009). AP24534, a pan-BCR-ABL inhibitor for chronic myeloid leukemia, potently inhibits the T315I mutant and overcomes mutation-based resistance. Cancer Cell *16*, 401–412.

Pao, W., Miller, V., Zakowski, M., Doherty, J., Politi, K., Sarkaria, I., Singh, B., Heelan, R., Rusch, V., Fulton, L., et al. (2004). EGF receptor gene mutations are common in lung cancers from "never smokers" and are associated with sensitivity of tumors to gefitinib and erlotinib. Proc. Natl. Acad. Sci. USA *101*, 13306–13311.

Pao, W., Miller, V.A., Politi, K.A., Riely, G.J., Somwar, R., Zakowski, M.F., Kris, M.G., and Varmus, H. (2005). Acquired resistance of lung adenocarcinomas to gefitinib or erlotinib is associated with a second mutation in the EGFR kinase domain. PLoS Med. *2*, e73.

Redaelli, S., Piazza, R., Rostagno, R., Magistroni, V., Perini, P., Marega, M., Gambacorti-Passerini, C., and Boschelli, F. (2009). Activity of bosutinib, dasatinib, and nilotinib against 18 imatinib-resistant BCR/ABL mutants. J. Clin. Oncol. *27*, 469–471.

Rodig, S.J., Mino-Kenudson, M., Dacic, S., Yeap, B.Y., Shaw, A., Barletta, J.A., Stubbs, H., Law, K., Lindeman, N., Mark, E., et al. (2009). Unique

clinicopathologic features characterize ALK-rearranged lung adenocarcinoma in the western population. Clin. Cancer Res. *15*, 5216–5223.

Sabbatini, P., Korenchuk, S., Rowand, J.L., Groy, A., Liu, Q., Leperi, D., Atkins, C., Dumble, M., Yang, J., Anderson, K., et al. (2009). GSK1838705A inhibits the insulin-like growth factor-1 receptor and anaplastic lymphoma kinase and shows antitumor activity in experimental models of human cancers. Mol. Cancer Ther. *8*, 2811–2820.

Saglio, G., Kim, D.W., Issaragrisil, S., le Coutre, P., Etienne, G., Lobo, C., Pasquini, R., Clark, R.E., Hochhaus, A., Hughes, T.P., et al. (2010). Nilotinib versus imatinib for newly diagnosed chronic myeloid leukemia. N. Engl. J. Med. *362*, 2251–2259.

Sasaki, T., Okuda, K., Zheng, W., Butrynski, J., Capelletti, M., Wang, L., Gray, N.S., Wilner, K., Christensen, J.G., Demetri, G., et al. (2010). The neuroblastoma-Associated F1174L ALK mutation causes resistance to an ALK kinase inhibitor in ALK-translocated cancers. Cancer Res. *70*, 10038–10043.

Sequist, L.V., Besse, B., Lynch, T.J., Miller, V.A., Wong, K.K., Gitlitz, B., Eaton, K., Zacharchuk, C., Freyman, A., Powell, C., et al. (2010). Neratinib, an irreversible pan-ErbB receptor tyrosine kinase inhibitor: results of a phase II trial in patients with advanced non-small-cell lung cancer. J. Clin. Oncol. *28*, 3076–3083.

Smolen, G.A., Sordella, R., Muir, B., Mohapatra, G., Barmettler, A., Archibald, H., Kim, W.J., Okimoto, R.A., Bell, D.W., Sgroi, D.C., et al. (2006). Amplification of MET may identify a subset of cancers with extreme sensitivity to the selective tyrosine kinase inhibitor PHA-665752. Proc. Natl. Acad. Sci. USA *103*, 2316–2321.

Soda, M., Choi, Y.L., Enomoto, M., Takada, S., Yamashita, Y., Ishikawa, S., Fujiwara, S., Watanabe, H., Kurashina, K., Hatanaka, H., et al. (2007). Identification of the transforming EML4-ALK fusion gene in non-small-cell lung cancer. Nature *448*, 561–566.

Soda, M., Takada, S., Takeuchi, K., Choi, Y.L., Enomoto, M., Ueno, T., Haruta, H., Hamada, T., Yamashita, Y., Ishikawa, Y., et al. (2008). A mouse model for EML4-ALK-positive lung cancer. Proc. Natl. Acad. Sci. USA *105*, 19893–19897.

Sos, M.L., Rode, H.B., Heynck, S., Peifer, M., Fischer, F., Klüter, S., Pawar, V.G., Reuter, C., Heuckmann, J.M., Weiss, J., et al. (2010). Chemogenomic profiling provides insights into the limited activity of irreversible EGFR Inhibitors in tumor cells expressing the T790M EGFR resistance mutation. Cancer Res. *70*, 868–874.

Takeuchi, K., Choi, Y.L., Soda, M., Inamura, K., Togashi, Y., Hatano, S., Enomoto, M., Takada, S., Yamashita, Y., Satoh, Y., et al. (2008). Multiplex reverse transcription-PCR screening for EML4-ALK fusion transcripts. Clin. Cancer Res. *14*, 6618–6624.

Takeuchi, K., Choi, Y.L., Togashi, Y., Soda, M., Hatano, S., Inamura, K., Takada, S., Ueno, T., Yamashita, Y., Satoh, Y., et al. (2009). KIF5B-ALK, a novel fusion oncokinase identified by an immunohistochemistry-based diagnostic system for ALK-positive lung cancer. Clin. Cancer Res. *15*, 3143–3149.

Tamborini, E., Bonadiman, L., Greco, A., Albertini, V., Negri, T., Gronchi, A., Bertulli, R., Colecchia, M., Casali, P.G., Pierotti, M.A., et al. (2004). A new mutation in the KIT ATP pocket causes acquired resistance to imatinib in a gastrointestinal stromal tumor patient. Gastroenterology *127*, 294–299.

Tomida, M., Ohtake, H., Yokota, T., Kobayashi, Y., and Kurosumi, M.J. (2008). Stat3 up-regulates expression of nicotinamide N-methyltransferase in human cancer cells. J. Cancer Res. Clin. Oncol. *134*, 551–559.

Weisberg, E., Manley, P.W., Breitenstein, W., Bruggen, J., Cowan-Jacob, S.W., Ray, A., Huntly, B., Fabbro, D., Fendrich, G., Hall-Meyers, E., et al. (2005). Characterization of AMN107, a selective inhibitor of native and mutant Bcr-Abl. Cancer Cell *7*, 129–141.

Wong, D.W., Leung, E.L., Wong, S.K., Tin, V.P., Sihoe, A.D., Cheng, L.C., Au, J.S., Chung, L.P., and Wong, M.P. (2011). A novel KIF5B-ALK variant in non-small cell lung cancer. Cancer, in press.

Zauberman, A., Lapter, S., and Zipori, D. (2001). Smad proteins suppress CCAAT/enhancer-binding protein (C/EBP) beta- and STAT3-mediated transcriptional activation of the haptoglobin promoter. J. Biol. Chem. *276*, 24719–24725.

Zhou, W., Ercan, D., Chen, L., Yun, C.H., Li, D., Capelletti, M., Cortot, A.B., Chirieac, L., Iacob, R.E., Padera, R., et al. (2009). Novel mutant-selective EGFR kinase inhibitors against EGFR T790M. Nature *462*, 1070–1074.